

CFD MODELING OF THE STEADY-STATE MOMENTUM AND OXYGEN TRANSPORT IN A BIOREACTOR THAT IS DRIVEN BY AN AERIAL ROTATING DISK

K. Y. S. LIOW* and B. T. TAN†

School of Engineering, Monash University, Malaysia

**keith.liow@eng.monash.edu.my*

†*tan.boon.thong@eng.monash.edu.my*

G. A. THOUAS

Division of Biological Engineering, Monash University, Australia

George.thouas@eng.monash.edu.au

M. C. THOMPSON

Department of Mechanical Engineering, Monash University, Australia

mark.thompson@eng.monash.edu.au

Received 13 March 2008

Revised 23 June 2008

This work considers the momentum transport and mass transfer of O_2 in a novel aerial rotating disk bioreactor (RDB) for animal cell or tissue culture. Specifically, this design uses a rotating lid placed above the surface of the culture medium to provide a stirring mechanism, which has potential benefits of enhanced gas transfer, reducing possible contamination, and better access to the culture medium below. The aim of this study is to use CFD to characterize the flow field, shear stresses, and oxygen profiles at a range of Reynolds number that lies within the laminar flow regime. Ultimately, such data will aid the development of an aerial RDB for tumor progression. Numerical simulation is used whereby the two-phase flow, comprising air as the gaseous phase, and water as the aqueous phase, is obtained by solving the unsteady, axisymmetric, incompressible Navier Stokes equation. Having obtained an accurate flow field, a species transport equation is then used to predict the oxygen transfer from the gaseous phase to the aqueous phase. Results are presented for a rotation Reynolds number (Re) range that corresponds to the impeller speed range of 60 to 240 rpm. While the flow is primarily swirl-dominant, it is found that the secondary flow in the aqueous region consists of a single recirculation pattern. As the oxygen transfer in the aqueous phase is mainly driven by convection, there is a clear depletion of oxygen at the center of the recirculation region. Shear stress distributions along the bottom stationary wall indicate a shift in the peak towards the external cylinder wall with increasing Re .

Keywords: Bioreactor; computational fluid dynamics; oxygen transfer; tissue engineering.

1. Introduction

Bioreactor processing hardware for tissue engineering continues to be an area of active research, not least in the development of optimum conditions for the *in vitro* culturing environment to stimulate and enhance cell or tissue growth. While bioreactor design considerations are extensive and varied, the three important factors in the research and pre-clinical stage (and possibly leading to scale-up) are as follows: appropriate levels of local shear stresses, adequate nutrients and oxygen supply, and waste elimination. It is commonly known that a dynamic system, usually via mechanical agitation, is preferred over a static type as both mixing and transport of nutrients to the cells are improved. The turbulent stirred (or spinner-flask) bioreactor is one common example of a dynamic bioreactor.¹

This study is a part of an ongoing research and development at Monash University that focuses on the laminar spinner-flask bioreactor as a possible alternative to the turbulent spinner-flask bioreactor. Amongst others, a novel stirred bioreactor that is operating under the laminar flow regime in the culture of EL-4 lymphoma cells has been used.² From the fluid dynamics perspective, the laminar bioreactor continues to receive attention both numerically and experimentally.³⁻⁵ It is worthwhile noting that these studies were performed at conditions that resulted in the formation of a vortex breakdown (VB) bubble. In particular, an interesting finding was the observation that the VB bubble was relatively rich in oxygen concentration.^{4,5}

Given that oxygen is the key ingredient in aerobic processes taking place in cell or tissue cultures, an important aim of this study is to model the oxygen diffusion taking place in the aerial rotating disk bioreactor (RDB). The novelty of this particular bioreactor comes from the fact that the disk/impeller that is driving the culture media is not in direct physical contact with the aqueous phase (refer to the schematic in Fig. 1(a)). In other words, the impeller is driving the gaseous phase while agitation of the aqueous phase is caused by its shearing effect on the moving air above it. The simulated streamlines corresponding to the secondary flow is shown in Fig. 1(b), whereby two recirculation regions exist in the gaseous phase, of which the bottom-located zone is driving the fluid, thereby resulting in a third recirculation region in the aqueous phase.

The non-contact of the impeller and the aqueous phase/culture media is important not only from the cell culture technological perspective in reducing potential contamination risks, but can also potentially provide enhanced gas transport and more direct access to the culture medium below.

Table 1 shows the geometrical specifications of the RDB that is modeled in this study. Here, the physical aspect ratios of the bioreactor are kept fixed at $H/R = 2.0$ and $R_d/T_d = 1.75$, where H is the height of the fluid-phase, R is the radius of the bioreactor, while R_d and T_d denotes the impeller radius and thickness respectively. The reference Reynolds number, Re , is based on the properties of air (at a system temperature of 37°), the angular rotation of the impeller, Ω , and the radius of the

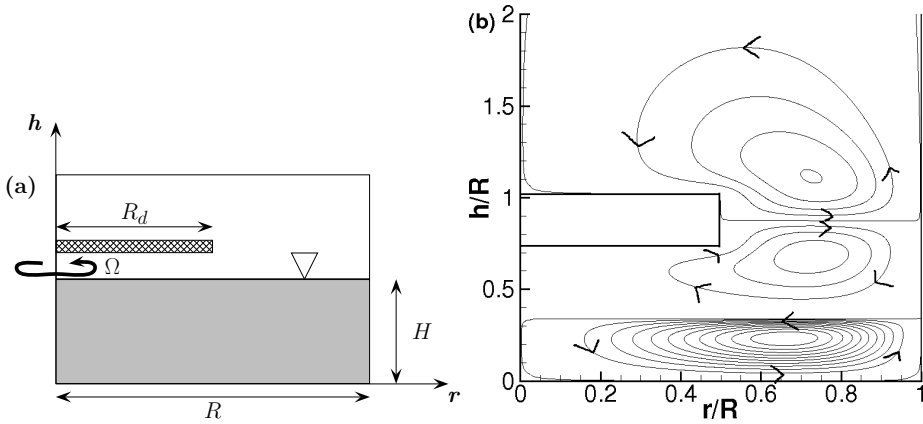


Fig. 1. (a) Schematic of the aerial RDB bioreactor in the (h, r) coordinate axes. Note that the schematic is not drawn to scale. (b) Simulated streamlines with arrows to denote the direction of rotation of the secondary flow in both phases.

Table 1. Specifications of the bioreactor configuration.

| | |
|---------------------------|--------------------------|
| Fluid-phase height, H | 6.00×10^{-3} m |
| Cylinder radius, R | 1.765×10^{-2} m |
| Impeller radius, R_d | 0.875×10^{-2} m |
| Impeller thickness, T_d | 5.00×10^{-3} m |

impeller, R_d . The hydrodynamic conditions and oxygen transfer taking place in the aerial RDB were studied by varying the angular rotation of the impeller at $\Omega = 60, 120$ and 240 rpm.

2. Numerical Method

The commercially available CFD software package, Fluent (version 6.3), was used to solve the incompressible, unsteady Navier–Stokes equations (INSE) in the 2D, axisymmetric reference frame. The species transport equation for oxygen in the aqueous phase is a scalar equation, and is decoupled from the INSE. Because we are only interested in the steady-state behavior, the multi-phase flow equations are first solved. Once the steady-state flow field has been obtained, the species transport equation for oxygen in the aqueous phase is then simulated to obtain the steady-state oxygen concentration field.

A first-order time-stepping scheme was used to march the simulations forward in time. The convective variables were discretized in space using the QUICK interpolation scheme while the SIMPLE algorithm was used for the pressure-velocity coupling. A spatial resolution study was conducted with the grid concentrated in regions with significant gradients (e.g., around the impeller, close to the stationary wall, and at the inter-phase boundary), and a non-dimensionalized spatial step-size

of $\Delta x/R_d = 5.0 \times 10^{-4}$ was used at the impeller boundaries, while at the inter-phase boundary, a grid spacing of $\Delta x/R_d = 1.0 \times 10^{-4}$ was used. It is expected that the inter-phase boundary will be relatively flat, nevertheless we have to ensure that the inter-phase curvature is adequately resolved to prevent spurious, unphysical oscillations from forming. It was also found that the timestep to achieve this was more restrictive than that required to march the flow to steady state. After a series of temporal tests, a timestep of $\Omega\Delta t/(2\pi) = 5.0 \times 10^{-4}$ was determined to be appropriate.

As the flow is assumed to be axisymmetric, the axis boundary condition is imposed at the inner radial boundary, $r = 0$. The no-slip condition is imposed at the side wall, $r = R$, and the bottom wall. At the fluid-gaseous interface, $z = H$, a free-surface condition is imposed, and the volume-of-fluids (VOF) approach is used.

The dilute approximation that assumes constant fluid-phase density and oxygen diffusivity, D , is used to solve the oxygen continuity equation (in terms of mass fraction, Y) in the fluid phase, and can be written as follows:

$$\frac{\partial Y}{\partial t} + \mathbf{V}\nabla \cdot Y = -D\nabla^2 Y + \gamma V_m.$$

This study assumes that the cells are uniformly suspended in the fluid-phase, and that the cells' oxygen consumption, γV_m , is of a zero-order reaction rate. While the Michaelis–Menten (MM) kinetics is probably a more realistic model that is indicative of the species consumption of cells, this study has assumed a zero-order reaction kinetics on the basis that the cell culture kinetics are extremely slow, and the regime described here is dominated by advection rather than diffusion. Furthermore, the scope of this study is limited to a time-independent case and as such, the oxygen concentration field is itself only a snapshot under equilibrated conditions. Nevertheless, the present findings would be moderated upon by a follow-up albeit more comprehensive study that also considers the transient state of the process of species consumption, and therefore the MM kinetics will be adopted.

As this study is only considering steady-state oxygen profiles, the fluid phase oxygen concentration at the free-surface can be assumed to be equal to the equilibrium concentration of saturated O_2 in the aqueous phase.⁶ This was calculated using Henry's law constant for dissolved oxygen in water at a user-defined system temperature of 37°C. As the aerial RDB is intended to be used for culturing the same cell line,² a molar oxygen consumption rate of $1.0\text{--}1.2 \times 10^{-17}$ mol $O_2/\text{m}^3\text{s}$ per cell was used.⁷ The zero oxygen flux condition was applied at the solid wall boundaries.

3. Results and Discussion

The numerical method used in this study to model the two-phase flow and the diffusion of oxygen from the gaseous phase to the aqueous phase is validated by an earlier published work⁸ that has considered a two-phase flow albeit with an impeller

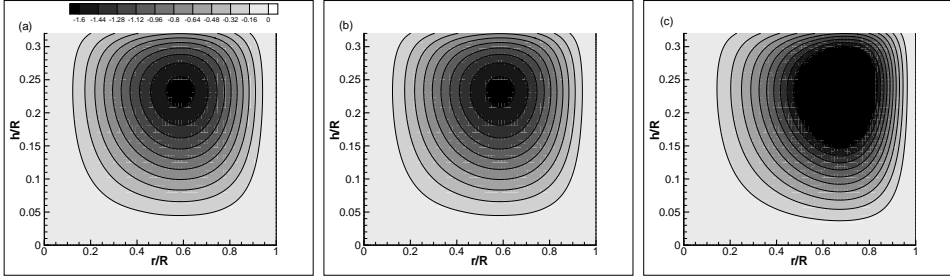


Fig. 2. Non-dimensionalized streamlines, $\Psi' = \Psi/(\Omega R_d^3)$, in the fluid phase corresponding to rotational speeds of (a) $\Omega = 60$ rpm, (b) $\Omega = 120$ rpm, and (c) $\Omega = 240$ rpm. The intervals are equally-spaced.

that is suspended inside the aqueous phase. In the earlier study, the numerical results were compared with experimental data³ and showed good agreement, both in qualitative behavior of the vortex breakdown topology and quantitative data such as shear stresses on the solid boundaries. These studies established the spatial resolution required to achieve predictive accuracy of a few percent. Direct validation of the results of the present study will be achieved in the near future, with experiments currently in progress.

Typically, the simulations took between 50–100 non-dimensionalized time units to reach an asymptotic state from zero-flow initialization. One non-dimensionalized time unit corresponds to one complete revolution of the impeller. The non-dimensionalized streamlines that are shown in Fig. 2 show that the rotating impeller imparts momentum to the gaseous phase, thereby resulting in two distinct recirculation regions, of which, the recirculation region directly underneath the impeller is driving the fluid into rotation via shear. From Fig. 1(a), the recirculation region underneath the impeller has a clockwise recirculation region. As a result, the fluid-phase has a anti-clockwise recirculation region. As the Reynolds number is increased, it is clear that there is increased momentum transfer across the gaseous fluid phase judging from the concentration of the streamlines close to the inter-phase surface.

Figure 3 shows the dimensionless oxygen concentration in the fluid-phase at the three different impeller rotation speeds. It is observed that oxygen is advected from the inter-phase surface towards the axisymmetric axis. As Fig. 3(a) shows, at the relatively low impeller speed of 60 rpm, oxygen is mainly diffused radially outwards. However, as the impeller speed is increased, the oxygen transport follows the recirculating pattern of the streamlines indicating the dominance of convection over diffusion. As a result, the center of the recirculation region has the lowest oxygen concentration (see Figs. 3(a) and 3(b)). This finding has good agreement with a previous work.⁵

In addition to the mass transfer, another important aspect of an increasing Reynolds number is its effect on the shear stresses along the bottom wall due to

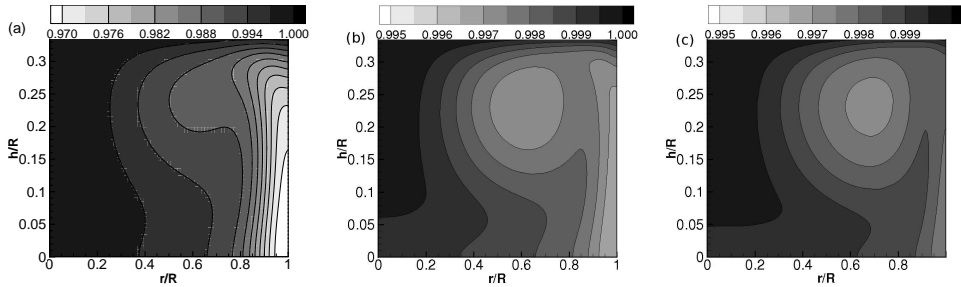


Fig. 3. Non-dimensionalized oxygen concentration corresponding to rotational speeds of (a) $\Omega = 60$ rpm, (b) $\Omega = 120$ rpm, and (c) $\Omega = 240$ rpm.

the eventual settling of the initially suspended cell aggregates. Figure 4 shows the radial distribution of the shear stresses on the bottom wall. It can be seen that the location of the peak stress moves radially outwards with increasing Re . The shear stress profile along the bottom wall of the bioreactor confirms previous simulations in higher aspect ratio volumes, indicating the scalability of the design despite the minor modifications.²

This result has several implications for standard cell culture methods. For instance, the method potentially allows for effective control of two-dimensional shear stresses at more physiological Reynolds numbers (1–100). This has potential advantages as a model to assess the biological effects of controlled mechanical stresses on anchorage-dependent cells types immobilized in scaffolds, by simple variation of scaffold placement. A similar approach has been adopted in a rotating wall bioreactor, by scaffold placement along the sidewall.⁹

Overall, shear stresses in the aerial disc bioreactor are approximately three to four orders of magnitude lower than for other stirred bioreactors such as spinner flasks¹ or annular flow reactors.¹⁰ Importantly, the flow remains largely laminar, particularly near the bottom wall where suspended cells aggregates or carrier beads tend to accumulate.

4. Conclusion

In this study, we have considered the flow field and oxygen transfer in a novel aerial rotating disk bioreactor (RDB) for cell or tissue culture. The RDB was modeled at a laminar flow regime. At the range of rotation Reynolds number that was modeled, the fluid phase showed the presence of a single, primary recirculation region in the fluid-phase. The results has shown that the oxygen transport can be improved through convection as a result of the steady, robust recirculation region. An experimental study is currently being undertaken by the main authors to provide validation of the numerical results, and further directions in the development of this exciting bioreactor configuration.

Broadly-put, improved efficiency of oxygen mass transport represents an ongoing issue in bioreactor design.¹¹ Our variant achieves this, but not at the expense of

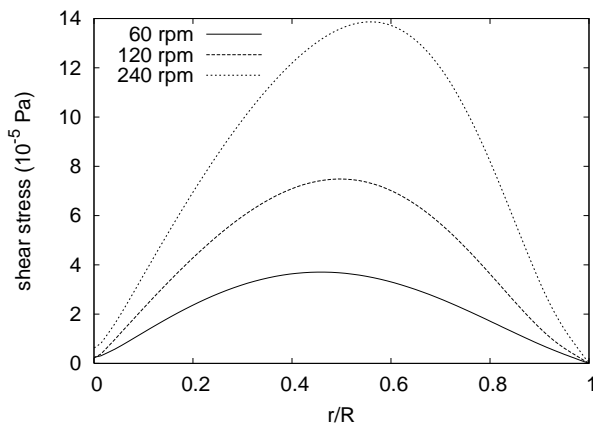


Fig. 4. Radial distribution of the shear stress along the bottom wall ($h = 0$).

excessive shear stress levels, and eliminates the need for direct fluid entrainment that interferes with the laminar flow regime. In practical terms, the bioreactor can be easily adapted to a standard static culture system, enabling it to be readily used for experimental or practical purposes in biotechnology laboratory settings.

References

1. P. Sucusky, D. F. Osorio, J. B. Brown and G. P. Neitzel, *Biotechnol. Bioeng.* **85** (2004) 34.
2. G. Thouas, J. Sheridan and K. Hourigan, *J. Biomed. Biotechnol.* **32754** (2007).
3. J. Dusting, J. Sheridan and K. Hourigan, *Biotech. Bioeng.* **94** (2006) 1196.
4. P. Yu, T. S. Lee, Y. Zeng and H. T. Low, *Mod. Phys. Lett. B* **19** (2005) 1543.
5. P. Yu, T. S. Lee, Y. Zeng and H. T. Low, *Comp. Methods Programs in Biomedicine* **85** (2007) 59.
6. K. A. Williams, S. Saini and T. M. Wick, *Biotechnol. Prog.* **18** (2002) 951.
7. V. L. Gabai, *FEBS* **329** (1993) 67.
8. K. Y. S. Liow, B. T. Tan, M. C. Thompson, K. Hourigan and G. A. Thouas, *16th Australasian Fluid Mechanics Conference* (2007).
9. H. Singh, S. H. Teoh, H. T. Low and D. W. Hutmacher, *J. Biotechnol.* **23** (2005); M. S. Croughan, J. F. Hamel and D. I. C. Wang, *Biotech. Bioeng.* **29** (1987) 130.
10. S. J. Curran and R. A. Black, *Biotechnol. Bioeng.* **30** (2005) 766.
11. M. Eisenstein, *Nat. Methods* **3** (2006) 1035.